The effective pair potential of expanded liquid caesium obtained by the inverse method

1997 J. Phys.: Condens. Matter 9 3303

(http://iopscience.iop.org/0953-8984/9/16/002)

J. Phys.: Condens. Matter **9** (1997) 3303–3312. Printed in the UK PII: S0953-8984(97)77209-6

The effective pair potential of expanded liquid caesium obtained by the inverse method

Shuji Munejiri, Fuyuki Shimojo, Kozo Hoshino and Mitsuo Watabe
Faculty of Integrated Arts and Sciences, Hiroshima University, Higashi-Hiroshima 739, Japan

Received 16 August 1996, in final form 10 October 1996

Abstract. The effective pair potentials $\phi(r)$ of liquid caesium for a wide range of density are derived from experimental structure factors using the inverse method, which is based on the integral equation theory and the molecular dynamics (MD) simulation. The results are discussed in comparison with those obtained previously for liquid rubidium and with those obtained by the pseudopotential perturbation theory. The density dependence of $\phi(r)$ derived for liquid caesium shows features in common with that for liquid rubidium: with decreasing density, the repulsive part of $\phi(r)$ becomes softer, its oscillation becomes smaller and then disappears and the resulting attractive part grows longer ranged. It is shown by comparing the corresponding states with the same scaled densities that the repulsive part of the $\phi(r)$ for caesium is softer than that for rubidium.

1. Introduction

As is well known, the interionic interaction in metals, which determines the arrangement of ions or the ionic structure, is the effective one in the sense that it contains the indirect ion–electron–ion interaction due to the screening effect of conduction electrons and hence depends on the density. Owing to this density dependence of the effective pair interaction, the structure of liquid metals changes more markedly with varying density than that of nonmetallic liquids, in which atoms or molecules interact through a density-independent potential.

As for liquid alkali metals, there occurs the metal–nonmetal transition near the critical point and consequently the cohesion mechanism of the system changes. At the ordinary liquid density near the triple point, the effective pair potential of these metals can be obtained by the pseudopotential perturbation theory based on the nearly-free-electron (NFE) model. On the other hand, the system in the gas phase is composed mainly of neutral atoms and molecules (and possibly some small numbers of ionized atoms and molecules and resultant free electrons), and the interaction potentials between these atoms and molecules are considered to be of the Lennard-Jones type. For the intermediate states near the critical point, however, there is no reliable theoretical method to derive the effective pair potential accurately. In fact, though the effective pair potential $\phi_{ps}(r)$ of liquid alkali metal obtained by the pseudopotential theory can reproduce the experimental structures very well at high densities near the triple point, it gives less satisfactory results at low densities near the critical point. Under these circumstances, it is interesting to investigate how the effective pair potential changes with the density, when the liquid alkali metal is expanded from the triple point to near the critical point along the liquid–vapour coexistence curve. So far this problem has not been solved.

0953-8984/97/163303+10$19.50

In this situation, one of the most effective approaches is the inverse method, in which the effective pair potential is derived from experimental structure factors. This approach was originally used by Johnson *et al* [1], and later several revised methods were proposed. More recently the predictor–corrector method for the inverse problem has been proposed by Reatto *et al* [2]; this is considered as the most reliable method at present. In our previous paper [3], we investigated the accuracy of this method and improved it in some points. Using this method we obtained the effective pair potentials $\phi(r)$ of liquid rubidium from the triple point to the state near the critical point, and investigated the density dependence of $\beta\phi(r)$ [4], where $\beta = 1/k_{\mathrm{B}}T$. The main results are as follows. Firstly, with decreasing density, the repulsive part of the effective pair potential $\beta\phi(r)$ becomes softer. Secondly the first peak and the oscillation of the $\beta\phi(r)$ disappear at low densities. Thirdly, while the depth of the minimum of $\beta\phi(r)$ becomes much shallower when temperature increases from 350 K to 900 K, it then remains almost unchanged from 900 K to 1700 K, and finally becomes shallower again when the temperature is raised further from 1700 K to 2000 K. This density dependence is qualitatively similar to that of the effective pair potentials $\beta\phi_{\mathrm{ps}}(r)$ obtained by the pseudopotential perturbation theory up to 1700 K but there appears an evident discrepancy between $\beta\phi(r)$ and $\beta\phi_{\mathrm{ps}}(r)$ at 2000 K.

The purposes of this paper are as follows: (i) we derive the effective pair potential $\phi(r)$ from the experimental structural data of liquid caesium for a wide range of density using the predictor–corrector method and investigate the density dependence of $\phi(r)$, (ii) we compare the results thus obtained with those for liquid rubidium explained above and (iii) we also compare the results with the effective pair potential $\phi_{\mathrm{ps}}(r)$ calculated by the pseudopotential perturbation theory.

2. Method of calculation

In the integral equation theory, we can obtain the effective pair potential $\phi(r)$ using the closure relation given by

$$\beta\phi(r) = g(r) - c(r) - \ln g(r) - 1 + B(r) \tag{1}$$

if we know the radial distribution function $g(r)$, the direct correlation function $c(r)$ and the bridge function $B(r)$. Therefore in order to obtain the effective pair potential from the experimental structure factor $S_{\mathrm{exp}}(k)$ using equation (1) we need the experimental radial distribution function $g_{\mathrm{exp}}(r)$, the experimental direct correlation function $c_{\mathrm{exp}}(r)$ and the experimental bridge function $B_{\mathrm{exp}}(r)$. The $g_{\mathrm{exp}}(r)$ can be obtained from $S_{\mathrm{exp}}(k)$ by the Fourier transformation

$$g_{\mathrm{exp}}(r) = 1 + \frac{1}{2\pi^2 nr}\int_0^\infty (S_{\mathrm{exp}}(k) - 1)k\sin(kr)\,\mathrm{d}k \tag{2}$$

where n is the number density of ions. Using the Ornstein–Zernike relation,

$$g(r) - 1 - c(r) = n\int (g(|\boldsymbol{r} - \boldsymbol{r}'|) - 1)c(r')\,\mathrm{d}\boldsymbol{r}' \tag{3}$$

together with equation (2), the $c_{\mathrm{exp}}(r)$ can also be obtained from the $S_{\mathrm{exp}}(k)$

$$c_{\mathrm{exp}}(r) = \frac{1}{2\pi^2 nr}\int_0^\infty \left(1 - \frac{1}{S_{\mathrm{exp}}(k)}\right)k\sin(kr)\,\mathrm{d}k. \tag{4}$$

The $B_{\mathrm{exp}}(r)$, however, cannot be obtained directly from $S_{\mathrm{exp}}(k)$. In the predictor–corrector method, we employ the bridge function of the hard-sphere system $B_{\mathrm{HS}}(r, \eta)$ as an initial estimate for $B_{\mathrm{exp}}(r)$, where the packing fraction η is determined so as to minimize the free

energy as is usually done in the modified hypernetted-chain (MHNC) approximation [5]. The condition [6] for the minimum free energy is given by

$$\int (g_{\rm exp}(r) - g_{\rm HS}(r,\eta)) \frac{\partial B_{\rm HS}(r,\eta)}{\partial \eta}\, {\rm d}\boldsymbol{r} = 0 \tag{5}$$

where $g_{\rm HS}(r,\eta)$ is the radial distribution function for the hard-sphere system. Thus the zeroth approximation for the effective pair potential is given by

$$\beta\phi_0(r) = g_{\rm exp}(r) - 1 - c_{\rm exp}(r) - \ln g_{\rm exp}(r) + B_{\rm HS}(r,\eta). \tag{6}$$

This approximation is called the predictor, and then $\phi_0(r)$ or $B_{\rm HS}(r,\eta)$ are improved by the following iterative procedure, which is called the corrector. (i) The simulation is performed with $\phi_i(r)$ $(= \phi_0(r)$ for the first run) and $g_i(r)$ is obtained, where i stands for the ith step. (ii) $S_i(k)$ is obtained by Fourier transforming $g_i(r)$. (iii) $c_i(r)$ is obtained by using equation (4), where the subscript exp is replaced by i. (iv) The revised bridge function $B_i(r)$ is given by

$$B_i(r) = \beta\phi_i(r) - g_i(r) + 1 + c_i(r) + \ln g_i(r). \tag{7}$$

An important point is that this bridge function $B_i(r)$ must be exact for the input effective pair potential $\phi_i(r)$, and if this condition is not satisfied, this iterative procedure would not converge. (v) The revised effective pair potential $\phi_{i+1}(r)$ is then given by

$$\beta\phi_{i+1}(r) = g_{\rm exp}(r) - 1 - c_{\rm exp}(r) - \ln g_{\rm exp}(r) + B_i(r). \tag{8}$$

The iterative process (i)–(v) is repeated until the difference $|\phi_{i+1}(r) - \phi_i(r)|$ becomes smaller than the desired accuracy and an accurate estimate for $\phi(r)$ can finally be obtained.

To carry out this predictor–corrector method, we must take into account the following points.

(I) In general the experimental structure factors $S_{\rm exp}(k)$ are available only in a limited-k region. The radial distribution function obtained by Fourier transforming the original experimental data of $S_{\rm exp}(k)$ is nonzero in the small-r region, where the $g_{\rm exp}(r)$ should be zero physically. Therefore in order to obtain $g_{\rm exp}(r)$ accurately, we have to extrapolate $S_{\rm exp}(k)$ both to larger- and to smaller-k regions. For the smaller-k region, we extrapolate the experimental data smoothly using spline functions to $S_{\rm exp}(0)$ obtained from the isothermal compressibility. As for the larger-k region, we perform the Fourier transform repeatedly between $S_{\rm exp}(k)$ and $g_{\rm exp}(r)$ until the unphysical structure of $g_{\rm exp}(r)$ in the small-r region is removed. In this way, we can get the 'experimental' structure factor for the whole k region. In the following the notation $S_{\rm exp}(k)$ is used to denote this extrapolated experimental structure factor. Since $g_{\rm exp}(r)$ and $c_{\rm exp}(r)$ are obtained from the same $S_{\rm exp}(k)$, these $g_{\rm exp}(r)$ and $c_{\rm exp}(r)$ satisfy the Ornstein–Zernike relation.

(II) As mentioned previously we must get the exact bridge function $B_i(r)$ at each step of the iterative procedure. To do so, we need first to obtain the data of $g_i(r)$ and $S_i(k)$ very accurately and then to get the $c_i(r)$ from the thus obtained $S_i(k)$. The values of $S_i(k)$ in the region where $S_i(k) < 1$ should be known very accurately to obtain the accurate values of $c_i(r)$, since, as is seen from equation (4), $c_i(r)$ is the Fourier transform of $(1 - 1/S_i(k))/n$, which contains the term $1/S_i(k)$, so the region where $S_i(k) \ll 1$ contributes substantially to the Fourier integral. Note that, near the triple point, $S_i(k)$ in the small-k region are much smaller than unity. For this reason, we need the accurate data of $g_i(r)$ in the large-r region, and therefore we must perform the simulation for a large system. Of course, at a low density near the critical point, the system size of the simulation must also be large, since the long-range correlation is important.

(III) Since $g_i(r)$ is obtained only for $r < L/2$, L being the side of the cubic cell used in the simulation, the data must be extrapolated to larger distances. We employ the Verlet extrapolation method [7], in which the Ornstein–Zernike relation is solved with the conditions that $g(r) = g_i(r)$ for $r < r_c$ and $c(r) = c_{PY}(r)$ for $r > r_c$, where $c_{PY}(r)$ is the direct correlation function in the Percus–Yevick (PY) approximation and r_c is the cutoff distance of $g_i(r)$.

3. Results and discussion

3.1. Experimental structural data

The structure factors for liquid caesium were measured by Winter *et al* [8] with neutron scattering for eight different thermodynamic states from the triple point to near the critical point along the liquid–vapour coexistence curve. To investigate the density dependence of the effective pair potentials, we choose the experimental structural data at 323, 573, 773, 1373 and 1673 K, where the corresponding observed densities are 1.83, 1.68, 1.57, 1.21 and 0.96 g cm^{-3}, respectively. These data are smoothed, extrapolated and modified as explained in the previous section. The values of $S_{exp}(k)$ and $g_{exp}(r)$ thus obtained are shown in figures 1 and 2, respectively and are used as input data in the inverse method. Note that, though these modified experimental structure factors $S_{exp}(k)$ are slightly different from the original experimental structure factors, the difference is within the experimental error. It is necessary to introduce this slight modification so as to produce the reasonable $g_{exp}(r)$ and $c_{exp}(r)$ which satisfy the Ornstein–Zernike relation. However, since the values of the modified $S_{exp}(k)$ are the same as the original experimental data in the small-k region, the difference mentioned above is not important for deriving the effective pair potential. With decreasing density, the main peak of $S_{exp}(k)$ becomes lower and broader and the $S_{exp}(k)$ in the small-k region becomes larger, reflecting large density fluctuation. As for the radial distribution function $g_{exp}(r)$, with decreasing density, the main peak position remains almost unchanged, while its height becomes lower. Note that, while functions $g_{exp}(r)$ for rubidium at 1700 K and 2000 K approach unity from above with damping oscillation [4], $g_{exp}(r)$ for caesium oscillates around unity at 1673 K and approaches unity from above at 1923 K. This behaviour reflects the large density fluctuation near the critical point and this feature has also been discussed theoretically [9].

It is known that the structure of liquids at high densities is mainly determined by the repulsive part of the pair potential and the attractive part has only a little effect on the structure. Therefore it is not easy to derive the attractive part of the effective pair potential from the experimental structure factor. As mentioned in the previous section, we need very accurate structure data in the small-k region to obtain the accurate effective pair potential, since $c_{exp}(r)$ is very sensitive to $S_{exp}(k)$ in this k region. Unfortunately the structure data near the triple point employed in this paper are not accurate enough to obtain the attractive part of the effective pair potential. In fact at 323 and 573 K, the effective pair potentials obtained by the inverse method depend strongly on the method of smoothing the raw experimental structure data in the small-k region. For this reason we will discuss in the following the density dependence of the effective pair potentials at 773, 1373 and 1673 K, where the $\phi(r)$ is not so sensitive to the experimental errors.

3.2. Effective pair potentials

We employ the constant-temperature molecular dynamics (MD) simulation [10, 11] in the predictor–corrector method. We take 4096 atoms in a cubic cell with the periodic boundary

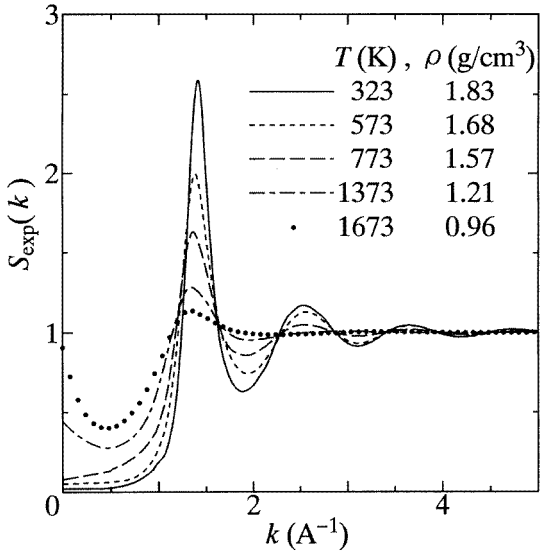

Figure 1. The extrapolated and modified structure factors $S_{\exp}(k)$ of liquid caesium at various temperatures.

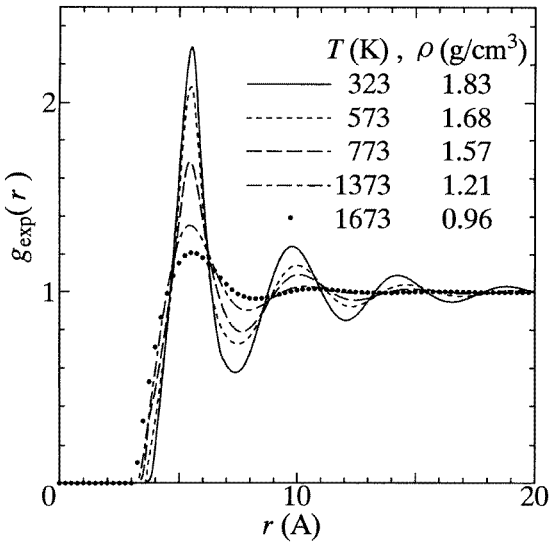

Figure 2. The experimental radial distribution functions $g_{\exp}(r)$ of liquid caesium obtained by the Fourier transform of the structure factors $S_{\exp}(k)$ shown in figure 1.

condition. The time step is 2.4×10^{-15} s. The length of a side of the cubic cell L is 83.2, 90.7 and 98.0 Å, the cutoff distance of the effective pair potential R_c is 15.0, 15.0 and 15.5 Å and the total number of simulation steps is 20 000, 110 000 and 160 000 at 773, 1373 and 1673 K, respectively. Note that the R_c values used here are large enough that the structure does not depend on R_c.

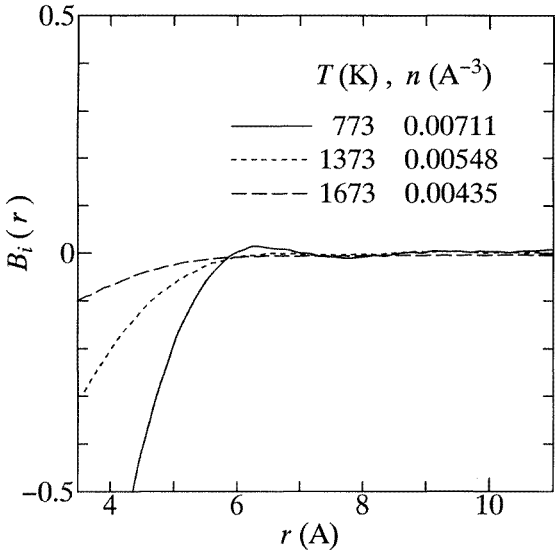

Figure 3. The bridge functions of liquid caesium $B_i(r)$ at three different states obtained by the inverse method, where $i = 1$ at 773 K and $i = 0$ at 1373 K and 1673 K.

The iteration procedure converges very rapidly; it is repeated twice at 773 K, and only once at 1373 K and 1673 K. The bridge functions obtained by this procedure are shown in figure 3. At low densities, since the contribution from the bridge function $B(r)$ is small, $\phi(r)$ does not depend so much on the approximation for the bridge function: indeed the effective pair potential revised by the corrector is not much different from that of the zeroth approximation. Therefore a few iterations are enough to achieve the convergence at these temperatures.

The effective pair potentials of liquid caesium obtained by the inverse method at three different states are shown in figure 4. The characteristic features of the density dependence of these potentials are as follows: (i) with decreasing density, the repulsive part of $\beta\phi(r)$ becomes softer, (ii) the oscillation and the resultant positive maximum around 8 Å of $\beta\phi(r)$ are clearly seen at 773 K but disappear at lower densities and (iii) the attractive part of $\beta\phi(r)$ becomes weaker and longer ranged as density decreases.

The feature (i) corresponds to the fact that the closest approach distance becomes shorter and the peaks of $g_{\exp}(r)$ become lower and broader with decreasing density. It should be noted here that the changes of both the closest approach distance and the amplitude of the oscillation of $g_{\exp}(r)$ are rather large and cannot be explained merely by the temperature effect. To confirm this, we performed the MD simulation for the system at 1673 K using the potential $\phi(r)$ at 1373 K, and, in fact, obtained a longer closest-approach distance and larger oscillation of $g(r)$ than the actual ones observed experimentally at 1673 K.

The wavelength of the oscillation of $\beta\phi(r)$ at 773 K is about 5 Å and this length agrees well with the corresponding wavelength of the Friedel oscillation 5.3 Å. The feature (ii) suggests that the system starts to deviate from the NFE-like metallic state, since the oscillation of the effective pair potential is a typical character of such a metallic state. In order to get the density at which the positive maximum of $\beta\phi(r)$ disappears, we calculated the $c_{\exp}(r)$ for all states using all the experimental structural data obtained by Winter *et al* [8]. As a result we found that the first minimum of the direct correlation function disappears

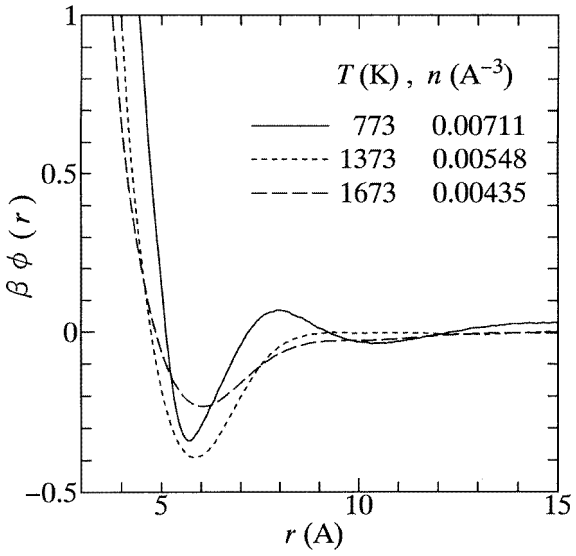

Figure 4. The effective pair potentials $\beta\phi(r)$ of liquid caesium obtained by the inverse method. The iteration procedure in the predictor–corrector method is done twice at 773 K and once at 1373 K and 1673 K.

between 973 K and 1173 K, and hence the first maximum of the $\beta\phi(r)$ disappears in the same temperature region. Note that the relation $c(r) = -\beta\phi(r)$, which is exact for $r \to \infty$, holds approximately even in the r region we are concerned with.

In order to check how and to what extent the weak and long-ranged attractive part of $\phi(r)$ affects the ionic structure at a low density, we have performed the MD simulation using $\phi(r)$ at 1673 K with the shorter cutoff length $R_c = 10.0$ Å. The structure factor thus obtained is clearly different from $S_{exp}(k)$ particularly in the small-k region where the calculated structure factor is significantly smaller than $S_{exp}(k)$. Since the difference is much larger than the experimental error, the weak and long-ranged attractive force derived by the present inverse method, though rather small, is considered to be indispensable.

At a low density, $S_{exp}(k)$ in the low-k region becomes large. It is well known that the repulsive part of $\beta\phi(r)$ plays a role of decreasing the structure factor in the small-k region, while its attractive part plays the opposite role [12]. It has been said so far that the role of the attractive force increases with decreasing density. In our results, although both the repulsive and the attractive forces become weaker as the density decreases, the degree of the softening of the repulsive force is so large that the effect of the attractive force becomes relatively stronger. The features (i) and (iii) reflect the increase of the structure factor in the long-wavelength region and we find that not only the weak and long-range attractive force but also the soft repulsive force have important effects on the structure at low density.

3.3. Comparison with the effective pair potentials of rubidium

Since we have already obtained the effective pair potentials for liquid rubidium [4] for a wide range of density and discussed their density dependence, it is interesting to compare the results of caesium with those of rubidium. We also compare these effective pair potentials obtained by the inverse method with those obtained by the pseudopotential perturbation

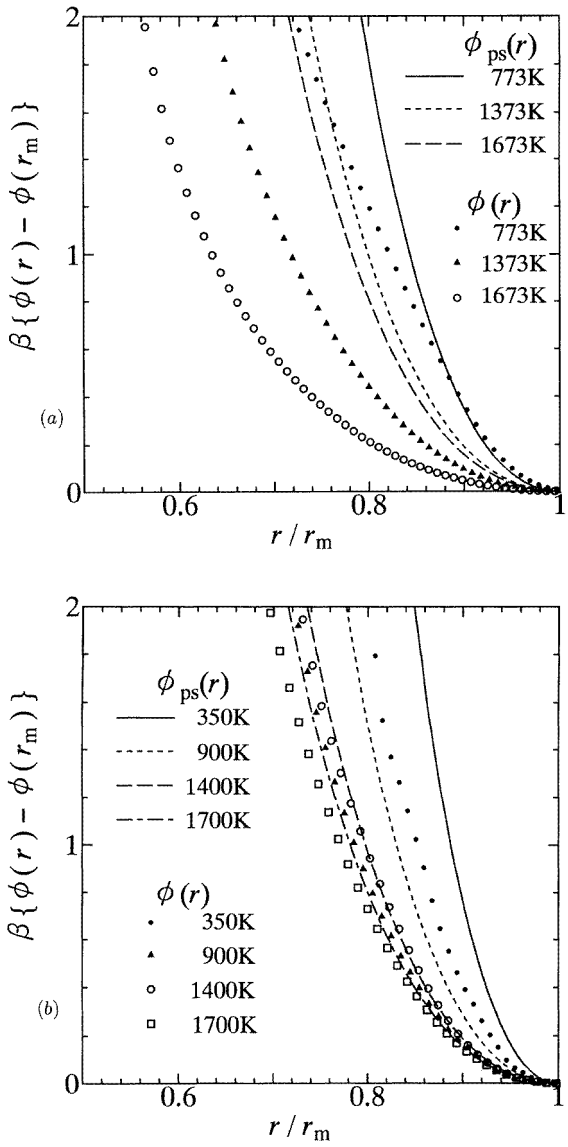

Figure 5. The density dependence of the repulsive part $\beta\{\phi(r) - \phi(r_m)\}$ for (*a*) Cs and (*b*) Rb, where r_m is the position of the first minimum of the $\phi(r)$. For comparison $\phi_{ps}(r)$ are also shown.

theory. As for the characteristic features (i), (ii) and (iii) discussed in 3.2, the effective pair potentials for liquid rubidium show the same density dependence as that for liquid caesium.

For closer comparison, the repulsive part of the effective pair potential defined as $\beta\{\phi(r) - \phi(r_m)\}$ for caesium and that for rubidium are shown in figure 5(a) and 5(b), respectively, where r_m is the position of the minimum of the $\phi(r)$. The repulsive part from 0.5 to 1.5 is fitted by the inverse power function A/r^m, A being a constant, using the least-squares method. For caesium m =7.7, 6.8 and 5.6 at 773, 1373 and 1673 K, respectively.

For rubidium, m =12.4, 9.6, 9.2 and 8.3 are obtained at 350, 900, 1400 and 1700 K, respectively. Here the states of liquid caesium at 773, 1373 and 1673 K approximately correspond to those of liquid rubidium at 900, 1400 and 1700 K, respectively, in the sense that n/n_c and T/T_c, where n_c is the critical number density and T_c the critical temperature, of these corresponding states are almost equal. Thus it is concluded from the comparison of the m values of these corresponding states that the repulsive part of $\beta\phi(r)$ for liquid caesium is softer than that for liquid rubidium. These results are in accordance with the following facts. If we compare the experimental structure factor $S_{exp}(k)$ with that of the hard-sphere system, with the hard-sphere diameter chosen so as to fit the height of the first peak of $S_{exp}(k)$, the agreement is very good for the rubidium except in the long-wavelength region, where the lack of the attractive force in the hard-sphere model becomes serious. As for caesium, on the other hand, it is difficult to fit the experimental structure factor using the hard-sphere model, even for the position of the first peak. These facts suggest that the effective pair potential of the caesium is softer than that of the rubidium.

Next we compare $\phi(r)$ with the effective pair potentials $\phi_{ps}(r)$ obtained by the pseudopotential perturbation theory, where the empty core potential of Hasegawa *et al* [13] and the local-field correction by Ichimaru and Utsumi [14] are used. The repulsive part of $\beta\phi(r)$ for caesium is softer than the corresponding $\beta\phi_{ps}(r)$ and the difference between them becomes larger as the density decreases. The difference of the repulsive part between $\beta\phi_{ps}(r)$ and $\beta\phi(r)$ of rubidium is qualitatively similar to that for caesium, though the former is quantitatively much smaller than the latter.

It is well known that dipole–dipole interaction between ion cores has an effect of softening the pair potential [15, 16]. Since the ionic polarizability of caesium is larger than that of rubidium, the softening effect is also expected to be larger for caesium than that for rubidium. Following Mon *et al* [16], we calculate the dipole–dipole interaction, and investigate the density dependence of the effective pair potentials which include the dipole–dipole interaction. As a result, we find that, though the dipole–dipole interaction between ions makes the effective pair potential soft, the effect is too small quantitatively to explain the results obtained by the inverse method.

It should be noted that the pair potential $\phi(r)$ derived from the experimental structure factors by the inverse method is, in general, an 'effective' potential which includes not only a pair interaction but also many-body interactions and therefore the $\phi(r)$ is not always comparable with the $\phi_{ps}(r)$, which is purely a pair potential.

4. Summary

We have derived the effective pair potentials of expanded liquid caesium using the inverse method and investigate their density dependence over a wide range of densities along the liquid–vapour coexistence curve. The characteristic features of the $\beta\phi(r)$, which is the effective pair potential scaled by temperature, are as follows. With decreasing density the repulsive part of $\beta\phi(r)$ becomes softer, the oscillatory behaviour of $\beta\phi(r)$ disappears and the attractive part of the $\beta\phi(r)$ becomes weaker and longer ranged. These features are the same as those known for liquid rubidium. Quantitatively, however, the repulsive part of $\beta\phi(r)$ is softer in caesium than in rubidium. It was also shown that the effective pair potentials obtained by the present inverse method are softer than the corresponding ones calculated by the pseudopotential perturbation theory and the difference between them for caesium is larger than that for rubidium.

Acknowledgment

This work is supported by a grant-in-aid for scientific research on priority areas (No 07236102) from the Ministry of Education, Science and Culture.

References

[1] Johnson M D, Hutchinson P and March N H 1964 *Proc. R. Soc.* A **282** 283
[2] Reatto L, Levesque D and Weis J J 1986 *Phys. Rev.* A **33** 3451
[3] Munejiri S, Shimojo F, Hoshino K and Watabe M 1995 *J. Phys. Soc. Japan* **64** 344
[4] Munejiri S, Shimojo F, Hoshino K and Watabe M 1996 *J. Non-Cryst. Solids* at press
[5] Rosenfeld Y and Ashcroft N W 1979 *Phys. Rev.* A **20** 1208
[6] Lado F, Foiles S M and Ashcroft N W 1983 *Phys. Rev.* A **28** 2374
[7] Verlet L 1968 *Phys. Rev.* **165** 201
[8] Winter R, Hensel F, Bodensteiner T and Gläser W 1987 *Ber. Bunsenges. Phys. Chem.* **91** 1327
[9] Matsuda N, Mori H, Hoshino K and Watabe M 1991 *J. Phys.: Condens. Matter* **3** 827
[10] Nosé S 1984 *Mol. Phys.* **52** 255
[11] Nosé S 1984 *J. Chem. Phys.* **81** 511
[12] Matsuda N, Hoshino K and Watabe M 1990 *J. Chem. Phys.* **93** 7350
[13] Hasegawa M, Hoshino K, Watabe M and Young W H 1990 *J. Non-Cryst. Solids* **117&118** 300
[14] Ichimaru S and Utsumi K 1981 *Phys. Rev.* B **24** 7385
[15] Rehr J J, Zaremba E and Kohn W 1975 *Phys. Rev.* B **12** 2062
[16] Mon K K, Ashcroft N W and Chester G V 1979 *Phys. Rev.* B **19** 5103